Synthesis and experiment of a lower limb exoskeleton rehabilitation robot

Jian Li
Beijing Key Laboratory of Rehabilitation Technical Aids for Old-Age and Disability and Key Laboratory of Intelligent Control and Rehabilitation Technology of the Ministry of Civil Affairs, National Research Center for Rehabilitation Technical Aids, Beijing, China and Robotic Institute, School of Mechanical Engineering and Automation, Beihang University, Beijing, China
Diansheng Chen
Robotics Institute, School of Mechanical Engineering and Automation, Beihang University, Beijing, China
Chunjing Tao
Beijing Key Laboratory of Rehabilitation Technical Aids for Old-Age and Disability and Key Laboratory of Intelligent Control and Rehabilitation Technology of the Ministry of Civil Affairs, National Research Center for Rehabilitation Technical Aids, Beijing, China, and
Hui Li
Shenzhou Tire Co. Ltd, Ningxia, China

Abstract
Purpose – Many studies have shown that rehabilitation robots are crucial for lower limb dysfunction, but application of many robotics have yet to be seen to actual use in China. This study aimed to improve a lower limb rehabilitation robot by details improving and practical design.
Design/methodology/approach – Structures and control system of a lower limb rehabilitation robot are improved in detail, including joint calculations, comfort analysis and feedback logic creation, and prototype experiments on healthy individuals and patients are conducted in a hospital.
Findings – All participating subjects did not experience any problems. The experiment shows detail improving is reasonable, and feasibility of the robot was confirmed, which has potential for overcoming difficulties and problems in practical application.
Research limitations/implications – Therapeutic effects need to be evaluated in the future. Also, more details should be improved continuously based on the actual demand.
Originality/value – The improved robot could assist the lower limb during standing or walking, which has significance for practical application and patients in China.

Keywords Ease of use, Rehabilitation robot, Details improving, Lower limb dysfunction, Robot application

Paper type Research paper

1. Introduction

Lower limb dysfunction (LLD) does not only lead to disability but also causes great inconvenience and is a burden to the families. The causes for LLD include spinal cord injury, traumatic brain injury, stroke, cerebral palsy and others. In particular, stroke can cause long-term disability. In China, patients suffering from stroke increase by about two million every year. Seven million stroke patients currently live in China (Zhao, 2014), of which about 4.5 million patients are unable to take care of themselves. Moreover, the disability rate caused by stroke is up to 75 per cent. Accoto *et al.* (2013) proposed that the rehabilitation of LLD can be divided into three phases:

1 A bedridden patient is mobilized into the bed or wheelchair as soon as possible.
2 A hospital patient needs to stand and restore gait by training.
3 A home patient uses rehabilitation aid for assistance.

Therefore, rehabilitation robots can be categorized into three types. First is the sitting/lying type, which is used in the early stage by bedridden patients [e.g. Erigo (Li *et al.*, 2011), MotionMaker (Swortec, Switzerland) and Lambda]. Second is the standing/walking type, which is used in the middle stage

The current issue and full text archive of this journal is available on Emerald Insight at: **www.emeraldinsight.com/0143-991X.htm**

Industrial Robot: An International Journal
44/3 (2017) 264–274

[DOI 10.1108/IR-10-2016-0255]

This work was supported in part by China Central-level Public research Institutes Fundamental Special Research under Grant 1181500900101 and National Key Technology Research and Development Program of the Ministry of Science and Technology of China under Grant 2009BAI71B03. The authors would like to thank the contributions of Can-jun Yang (Zhejiang University) and Lin-hong JI (Tsinghua University), as well as help from Guo-xin PAN, Xiufeng ZHANG, Run JI Zhong-jun MO and Jun-chao GUO.

Received 13 October 2016
Revised 12 December 2016
Accepted 13 December 2016

by hospital patients and usually incorporated with a partial body weight support (PBWS) system, such as Lokomat (Jezernik *et al.*, 2013), LokoHelp (LokoHelp Group, Germany), ReoAmbulator (Motorika, USA) and ALEX (Banala *et al.*, 2009). Third is the assisted walking type, which is used in the last stage by home patients and usually with two crutches or a walker for balance and protection [e.g. Rewalk (Esquenazi *et al.*, 2012), Hal (Kawamoto *et al.*, 2013), BLEEX, WSE (Onen *et al.*, 2012), Ekso™ (Joanne, 2014), PARGO (Chen *et al.*, 2015) and ATLAS (Sanz-Merodio *et al.*, 2014)]. Although none of the three types exhibit overwhelming superiority, the second type often attracts more attention from doctors and patients because of heavy physical labor. The first type is used when a patient is in the weakest situation. However, in China, this type has yet to be accepted because the Chinese believe that resting is of utmost importance based on traditional medicine theory. The third type often needs patients to buy the robot himself, not everyone can afford this, particularly if the robot is not included in their health insurance. Therefore, our research focused on the second type (Wang *et al.*, 2014).

With regard to the second type, although Lokomat, LokoHelp and ReoAmbulator have been successfully commercialized and utilized in clinics (Bonnyaud *et al.*, 2014), we have yet to see many robotics applied to practical health care in China because of the expensive price, inappropriate design and other reasons. For instance, Lokomat and LokoHelp use adjustable parallel bars as armrests, but height or width of armrest and exoskeletons should be adjusted separately, which spend more time. The morphology of parallel bars limits patients for wearing exoskeletons. ReoAmbulator uses open mechanism for armrests, but the width of the armrests cannot be adjusted and exoskeletons cannot move. Simultaneously, Hussain *et al.* (2016) proposed some limitations, such as the non-repetitive nature of training sessions and a lack of any objective method, to record and analyze. Hussain S. *et al.* have reviewed design and control problems of this type (Hussain *et al.*, 2011). Furthermore, most studies construct high-tech robots, and they have insufficiently paid attention to robotic applications (Geroin *et al.*, 2013), especially in terms of the details, such as difficulty in wearing and removing exoskeletons (Stegal *et al.*, 2013); high energy consumption of preparation and training; large space required for robots; restricted movement caused by robot's suspension vest; and long pre-preparation time for robot and patient.

Based on the above analysis, we investigated a standing/walking rehabilitation robot and noted detailed points for its design. A lower limb exoskeleton rehabilitation robot system (LLERRS) based on body weight support treadmill training (BWSTT) was designed. Some details and prototype tests are described, and results of healthy individuals and patients are analyzed to confirm the feasibility and function of LLERRS.

2. Methods

2.1 Detail improving

As shown in Figure 1, LLERRS is developed to assist LLD patients in performing both standing and walking, and following details are considered (Sui *et al.*, 2014):

Figure 1 Schematic of LLERRS

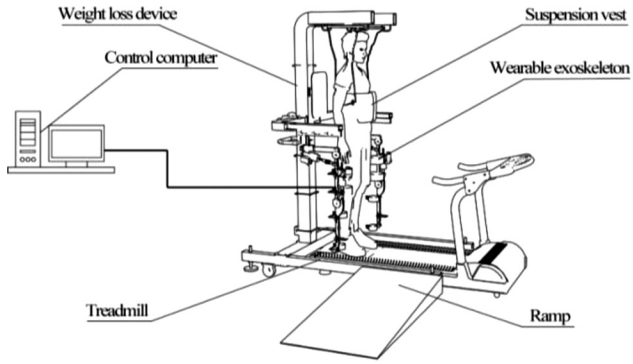

- Itineraries of ball screws for hip and knee are calculated to limit rotation angles of joints.
- Armrests of weight loss device could rotate to 90° such that a patient's wheelchair could easily go up and down the treadmill and the suspension vest is convenient to wear.
- Under the armrests, two sliding rails are present. Exoskeletons could slide back and forth for wear and removal.
- Comfort factors during lifting by weight loss device are analyzed to improve energy consumption.
- The suspension vest, which has an inverted triangle shape, could be divided into several parts so that patients could wear it in the wheelchair or on the treadmill.
- A simple closed-loop control system is built.
- Chinese people's habits and characteristics are emphasized throughout the design.

2.1.1 Joint calculation

The wearable exoskeletons have hip, knee and ankle joints (Pan *et al.*, 2014). From the perspective of application, only sagittal plane motion is considered and designed. The schematic of a designed exoskeleton with ball screws is illustrated in Figure 2 (Krishnan *et al.*, 2013).

Although the rotary motor that is directly placed on the joint point can approach the joint closely, it is simple to use. However, volume is limited, and rotation angle may exceed joint angle when the controls fail. Therefore, ball screws are applied to create joints because of high safety. We calculated the itineraries of ball screws for hip and knee (Yang *et al.*, 2014) to limit rotation angles and avoid secondary damage. As shown in Figure 3, hip joint includes hip motor, hip connector, thigh and hip ball screws. Its itinerary is calculated as follows:
In the initial state:

$$\begin{cases} D_1C^2 = AC^2 + AD_1^2 \\ D_1C = D_1M_1 + M_1B_1 \end{cases}. \quad (1)$$

In the forward swing state:

$$\begin{cases} D_2C^2 = AC^2 + AD_2{}^2 - 2AC \cdot AD_2 \cos\theta_{h\max} \\ D_2C = D_2M_2 + M_2B_2 + N_2C \end{cases}. \quad (2)$$

In the rear swing state:

Figure 2 Schematic of exoskeleton with ball screws and specific structural design (Guo *et al.*, 2014)

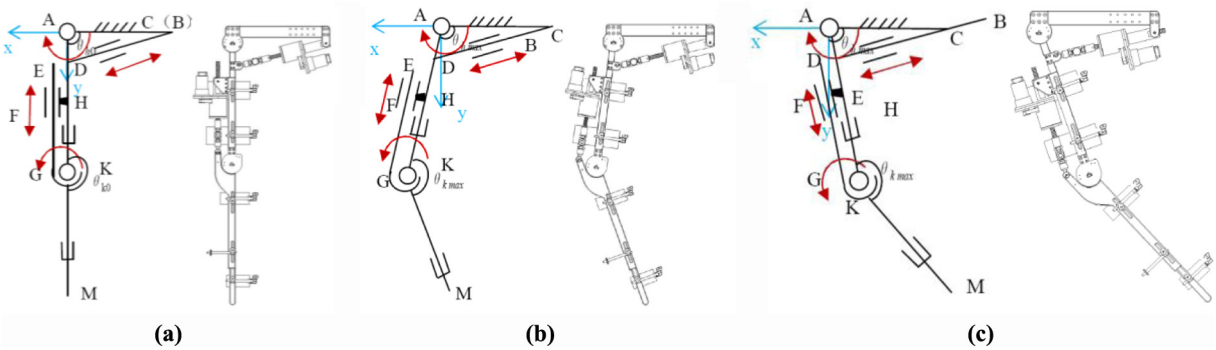

Notes: (a) Initial state; (b) forward swing state; (c) rear swing state

Figure 3 Hip joint of exoskeleton under three typical patterns

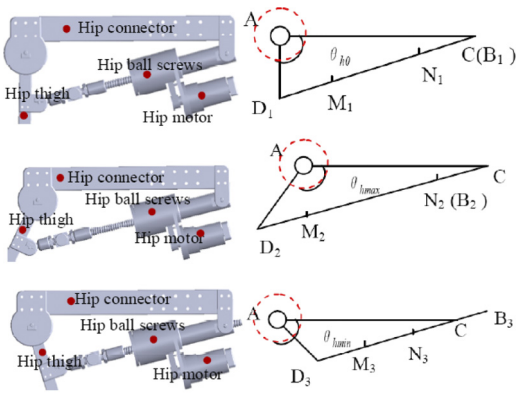

Note: The itinerary of ball screws changes with θ_h, which is the rotation angle of hip joint

$$\begin{cases} D_3C^2 = AC^2 + AD_3^2 - 2AC \cdot AD_3 \cos \theta_{h\min} \\ D_3C = D_3M_3 + M_3N_3 + N_3C \end{cases}, \quad (3)$$

where θ_{h0} is the initial angle for hip, which is 90°; $\theta_{h\max}$ is the maximum extension angle for hip; $\theta_{h\min}$ is the minimum flexion angle for hip; AC is the schematic of hip connector; and AD_1, AD_2 and AD_3 are parts of thigh in the initial state, forward swing state and rear swing state, respectively. AD_1, AD_2 and AD_3 have the same values with different coordinates. Similarly:

$$\begin{cases} D_1M_1 = D_2M_2 = D_3M_3 \\ N_1C = N_2C = N_3C \end{cases}. \quad (4)$$

The values of M_1N_1, M_2N_2 and M_2N_2 differ because the position of B changes with thigh swing. Given that the minimum value of M_3N_3 is decided by $L_{h\text{-}screwnut}$, which is the width of hip screw nut, and $L_{h\text{-}screwnut}$ is known when exoskeleton is designed, we can combine equations (1), (2), (3) and (4) to obtain:

$$\begin{cases} DM = D_3C - L_{h\text{-}screwnut} - D_2C + D_1C \\ NC = D_2C - D_1C \\ \Delta L_{h\text{-}screwnut} = D_2C - D_3C + L_{h\text{-}screwnut} \end{cases}. \quad (5)$$

The values of AC, AD, $\theta_{h\max}$ and $\theta_{h\min}$ are known, so D_1C, D_2C and D_3C can be determined using equations (1), (2) and (3), respectively. Finally, DM, NC and $\Delta L_{h-screw}$ can be obtained by equation (5), where $\Delta L_{h-screw}$ is the maximum safe itinerary of hip ball screws, and DM and NC are the lengths of connectors for ball screws.

Similarly, knee joint includes knee motor, knee connector, crus and knee ball screws. Based on Figure 4, the itinerary calculation is as follows:

In the initial state:

$$HK = GF = G\mathcal{J}_1 + \mathcal{J}_1P_1 + P_1F. \quad (6)$$

In the forward swing state:

$$\begin{cases} \tan(\theta_{k\min l} - 90^0) = \dfrac{O_2K}{O_2G} = \dfrac{FH}{O_2G} \\ O_2G = \dfrac{FH}{\tan(\theta_{k\min l} - 90^0)} \\ O_2G + HK = \mathcal{J}_2P_2 + P_2F + G\mathcal{J}_2 \end{cases}. \quad (7)$$

In the rear swing state:

$$\begin{cases} \tan(\theta_{k\min r} - 90^0) = \dfrac{O_3K}{O_3G} = \dfrac{FH}{O_3G} \\ O_3G = \dfrac{FH}{\tan(\theta_{k\min r} - 90^0)} \\ O_3G + HK = \mathcal{J}_3F + G\mathcal{J}_3 \end{cases}, \quad (8)$$

where θ_{k0} is the initial angle for knee, which is 180°; $\theta_{k\max l}$ is the left maximum extension angle for knee; $\theta_{k\max r}$ is the right maximum flexion angle for knee; HK is part of the thigh; and FH, O_2G and O_3G have same values in the initial state, forward swing state and rear swing state, respectively. Similarly:

$$\begin{cases} P_1F = P_2F = P_3F \\ \mathcal{J}_1G = \mathcal{J}_2G = \mathcal{J}_3G \end{cases}. \quad (9)$$

Given that the minimum value of $P\mathcal{J}$ is also decided by $L_{k\text{-}screwnut}$, which is the width of knee screw nut, we can combine equations (6), (7), (8) and (9) to obtain:

Figure 4 Knee joint for exoskeleton under three typical patterns (Yan *et al.*, 2014)

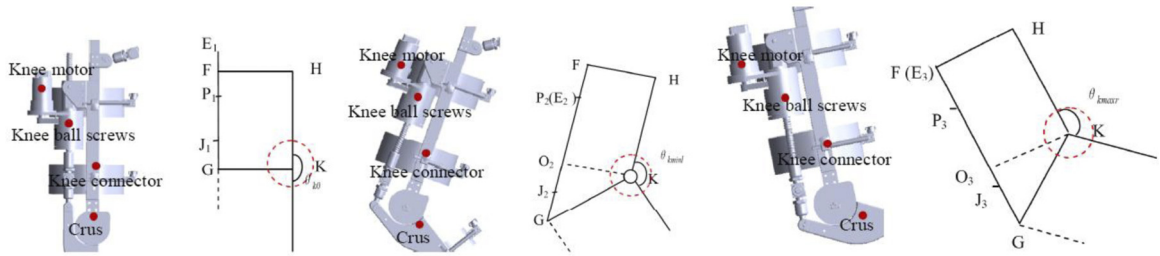

Note: The itinerary of ball screws changes with θ_k, which is the rotation angle of knee joint

$$\begin{cases} G\mathcal{J} = HK - L_{k-screwnut} - \dfrac{FH}{\tan(\theta_{k-\min-l} - 90^0)} + \dfrac{FH}{\tan(\theta_{k-\min-r} - 90^0)} \\ PF = \dfrac{FH}{\tan(\theta_{k-\min-l} - 90^0)} - \dfrac{FH}{\tan(\theta_{k-\min-r} - 90^0)} \\ \Delta L_{k-screw} = \dfrac{FH}{\tan(\theta_{k-\min-l} - 90^0)} + L_{k-screwnut} \end{cases} \tag{10}$$

The values of HK, $\theta_{k-\min-l}$, $\theta_{k-\min-r}$ and $L_{k\text{-}screw\ nut}$ are known, so $G\mathcal{J}$, PF and $\Delta L_{k-screw}$ can be obtained by equation (10), where $\Delta L_{k-screw}$ is the maximum safe itinerary of knee ball screws, and $G\mathcal{J}$ and PF are the lengths of connectors for knee ball screws. Both $\Delta L_{h-screw}$ and $\Delta L_{k-screw}$ offer final mechanical protection for patients when other security protocols fail to take effect.

2.1.2 Comfort analysis

Heavy counterweight or independent suspension mechanisms were used to adjust weight loss devices in past designs (Chen *et al.*, 2011). Such designs not only have huge volume but also are not conducive to actual operations. As shown in Figure 5, weight loss systems consist of armrests, frame, electric column and treadmill. PBWS system for LLERRS uses an electric column to lift people partially or completely. Two 90° rotating armrests are designed, which can provide support force and protection measures when a patient is standing and walking. Simultaneously, two sliding rails under corresponding armrests are created for wheelchairs to go up and down the treadmill, wearing exoskeletons and suspension vests. The height and width of the armrest and exoskeleton are adjusted according to individual characteristics. In addition, BWSTT usually needs to lift the body and reduce weight load on the lower limbs because patients are very weak who cannot stand by themselves. Therefore, keeping comfortable and improving energy consumption are important. Suspension can bring extra forces onto the body, and some force will bring discomfort and poor results when patients are lifted for a long time (Lu *et al.*, 2013). Thus, a force model (Figure 5) was established to improve the situation. When $\sum F_x = 0$ (F_x is horizontal force), $\sum F_y = 0$ (F_y is vertical force) and $\sum M = 0$ (M is torque), we can obtain:

$$\begin{cases} 2f_u + T_{2x} + S_{2x} + f_{f1} + f_{f2} = T_{1x} + S_{1x} \\ F_s + 2N_u + T_{1y} + T_{2y} + S_{1y} + S_{2y} + N_{f1} + N_{f2} = G + f_s \\ T_1 l_{T1} + S_1 l_{s1} + N_{f1} l_{Nf1} + f_u l_{fu} = \\ T_2 l_{T2} + S_2 l_{s2} + N_{f2} l_{Nf2} + N_u l_{Nu} + f_{f1} l_{f1} + f_{f2} l_{f2} \end{cases} \tag{11}$$

Figure 5 Force model for LLERRS with patients

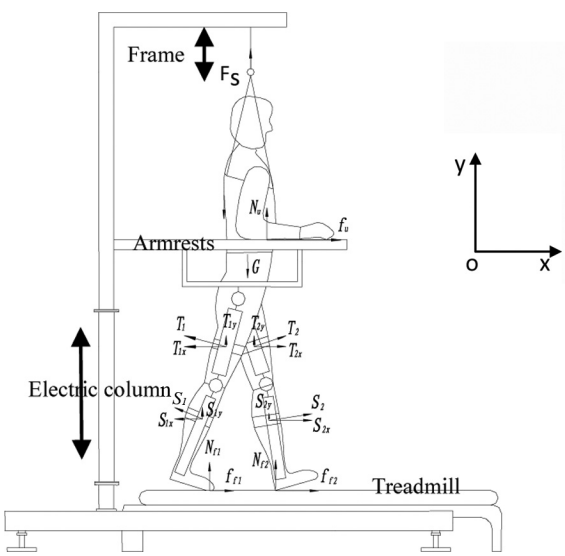

In equation (11), F_s is the lifting force that the suspension device gives to the body; f_s is the friction force that suspension vest gives to the body; N_u and f_u are the support force and horizontal friction force for patient's arm, respectively; T_{1x}, T_{2x}, T_{1y} and T_{2y} are the component forces that exoskeleton gives to the thigh in the x and y directions; S_{1x}, S_{2x}, S_{1y} and S_{2y} are the component forces that exoskeleton gives to the crus in the x and y directions; f_{f1}, f_{f2}, N_{f1} and N_{f2} are the normal forces and static friction forces for two feet; and l_{T1}, l_{S1}, l_{Nf1}, l_{fu}, l_{T2}, l_{S2}, l_{Nf2}, l_{Nu}, l_{f1} and l_{f2} are corresponding lever arms. When users are walking on the treadmill with exoskeletons, T_{1x}, T_{2x}, S_{1x}, S_{2x}, F_s, f_s, N_u, T_{1y}, T_{2y}, S_{1y} and S_{2y} have direct influences on the body's comfort. Among them, a relationship exists between F_s and f_s. When F_s is getting bigger, f_s may increase and people may feel discomfort. If f_s does not increase as F_s, suspension vest may slide into armpit. However, the armpit has numerous blood vessels, nerves and lymph. The upper limb will feel numb when armpits are oppressed for a certain time. For N_u, an accepted value can provide support

and safety to patients in a short time. However, in the long term, a large N_u may provide discomfort and lead to gravis of upper limbs. T_{1x}, T_{2x}, S_{1x}, S_{2x}, T_{1y}, T_{2y}, S_{1y} and S_{2y} are relatively stable for the same people. If the exoskeleton is light and the tightness between the lower limb and exoskeleton is appropriate, the patient will feel comfortable during training.

When T_{1x}, T_{2x}, S_{1x} and S_{2x} are unchanged, a great F_s can lead to bigger f_s and smaller N_u and f_u. The patient's torso and armpit may feel uncomfortable, but upper forearm may feel even more comfortable. Assuming that the extent of comfort is constant, that is, N_u and f_u are unchanged, F_s, f_{f1}, f_{f2}, N_{f1} and N_{f2} will decrease when T_{1x}, T_{2x}, S_{1x} and S_{2x} will increase. In the perspective of weight loss, increasing the values of F_s, N_u, T_{1y}, T_{2y}, S_{1y} and S_{2y} may be a good idea. However, these changes may lead to some discomfort for the patient. Therefore, the sequence of the above factors for comfort is:

$$f_s > N_u > T_1 = T_2 = S_1 = S_2. \tag{12}$$

Based on the previous analysis, a feasible method is improving the interface of the suspension vest to prevent it from sliding into the armpit. To improve f_s and feeling when patient is suspended, two kinds of customized orthotics were made. As Figure 6(a) shows, two volunteers were lifted with inverted triangular force and thigh ischial force for more than 35 min. The blood pressure and heart rate of subjects are slight higher at the beginning, but all values are in the normal range. Based on the above explanation, an inverted triangle shape is selected for the novel suspension vest. Soft fabric material is used for the suspension vest. As shown in Figure 6(b), the new soft suspension vest has an inverted triangle shape that includes a torso vest and thigh harness. The whole lifting force is divided into four parts: F_{s1}, F_{s2}, F_{s3} and F_{s4}:

$$F_s = F_{s1} + F_{s2} + F_{s3} + F_{s4}, \tag{13}$$

where F_{s1} and F_{s2} are the torso forces, and F_{s3} and F_{s4} are the thigh forces which can reduce discomfort of patient. Simultaneously, torso pressure N_s may decrease because:

$$f_s = \mu N_s \sin\theta. \tag{14}$$

When N_s is reduced, friction force f_s will also decrease. Thus, the patient will feel comfortable and consume less energy. Moreover, tightness and angle of θ for the vest can be adjustable so that different people can use it comfortably.

2.1.3 Real-time feedback and control

Vicon motion capture system (Oxford Metrics Limited Company, UK) is used to collect joint information in normal gait to provide real-time optical data for the robot. In total, 20 healthy subjects (30 ± 5 years old) with heights of 160-180 cm and weights of 70 ± 10 kg are selected to participate in the research. Information such as power, force, moment and angle were obtained from the hip and knee.

As shown in Figure 7, original data are input into software and average processing is conducted to meet the majority of needs, and the results are used as standard data to guide joint motors. Meanwhile, standard data can be divided into several categories to meet different patients' needs, which can be selected during patient training.

A closed control system (Figure 8) was developed, which included a computer, controller, encoders, motor and control software. The whole control system was divided into master computer and slave computer. Standard data were stored for master computer controlling four motors on the exoskeletons by a controller area network. The slave computer provides a practice motor's position, angle, velocity and torque to master computer and displayed information on the screen in real time. When actual angle for hip and knee (θ_{Ha} or θ_{Ka}) exceeds the expected value (θ_H or θ_K), the system will automatically stop for protection. Meanwhile, time-training mode and step-training mode were established to meet the needs of different patients for real-time control. Time-training mode

Figure 6 Simple experiments and analysis for suspension vest

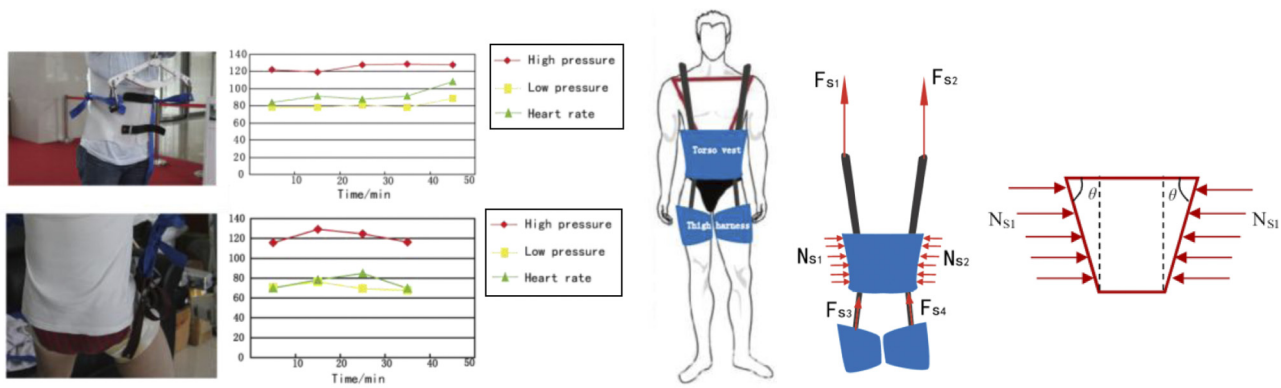

Notes: (a) Suspension experiment; (b) analysis of vest

Figure 7 Average processing of hip and knee's angle (Chen *et al.*, 2015)

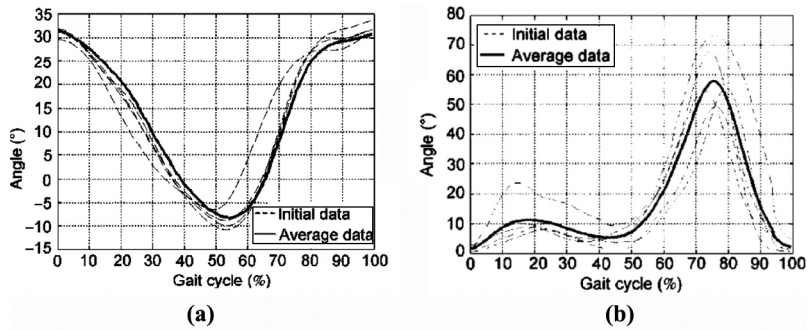

Notes: (a) Movement patterns of the hip joint; (b) movement patterns of the knee joint

Figure 8 Control algorithm of LLERRS

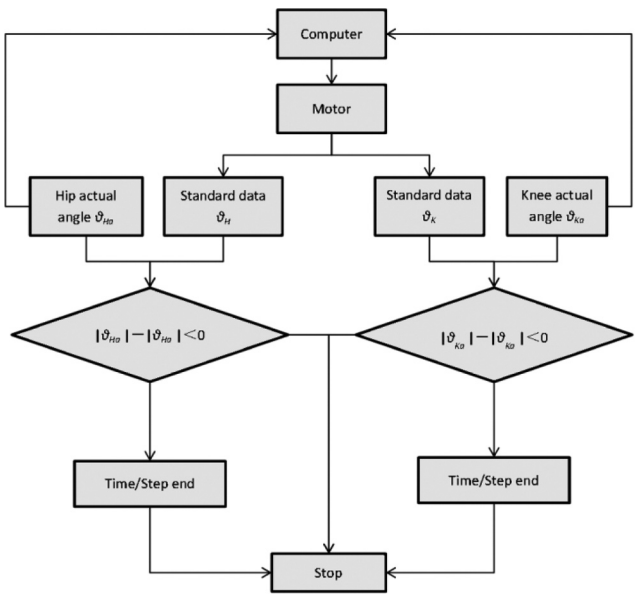

runs as the setting time. Once time arrives, LLERRS will stop directly. Step-training mode runs as the gait cycle. LLERRS will first enter the initial state (Figure 2) and then stop.

2.2 Functional experiment

To verify the usability of LLERRS, a prototype experiment was conducted in a hospital. All ethical issues with the experiment are in accordance with local ethical regulations. The experiment involved six healthy individuals (two female and four male) and two patients (male), whose details are listed in Table I.

2.2.1 Experiment on healthy individuals

Before patient training, five healthy volunteers and Doctor ZHAO [Figure 9(a)], who is chief physician of limb rehabilitation (40 years old, 162 cm tall and 55 kg in weight), tried LLERRS for 20 min. A speed of 0.5 mph was used during training, and the degree of weight loss was 80 per cent. Moreover, subjective feelings and objective experimental data are recorded in detail. During the experiment, the subjects were asked to relax their limbs, and then robot manipulated the lower limbs to complete standing or walking.

2.2.2 Experiment on patients

Based on the above experience, two young patients (one patient is a 20-year-old male, 175 cm tall and 62 kg in weight [Figure 9(b)]; his right leg lost the ability to walk because of encephalitis; the other patient is a 32-year-old male, 168 cm tall and 65 kg in weight; his legs lost the ability to walk because of brain damage by fighting) with different degrees of LLD but clear mind are selected for the experiment. The patients provided consent and agreed to train with LLERRS twice a day for 10 days completely free under the care of two doctors. Each training session lasted 20 min, and the velocity and degree of weight loss are 0.2 mph and 80 per cent, respectively.

3. Results and discussion

3.1 Results of healthy individuals

After experimenting on healthy individuals, we found that standing/walking function was satisfactory, but subjects were afraid of robot and movement of legs and exoskeletons was not coordinated at the first time. According to experience of subjects and doctor, we redesigned some parts, especially human–machine interface, such as soft contact surfaces of armrest, exoskeleton and vest. Psychological counseling from a doctor is necessary for patients before training, and slow velocity (<0.3 mph) is a good choice for a patient's first time.

As Figure 10(a) shows, objective data of position and velocity for hip and knee change periodically. We find that the response time of healthy individuals is less than 0.8 s. Moreover, movement of left leg and right leg demonstrates good consistency (Guo *et al.*, 2014). The time of one gait cycle is 1.8 s. As Figure 10(b) shows, most torques of right and left hips change regularly and correspond with each other during training. When left side reaches forward maximum, right side achieves reverse maximum. When left side reaches reverse maximum, right side achieves forward maximum. As Figure 10(c) shows, torques of right knee and left knee do not change regularly, and they demonstrate a 0.9 s time delay.

Table I Experiment details of healthy individuals and patients

Subjects	Gender	Age	Height (cm)	Weight (kg)	Training speed (mph)	Training time (min)	Subjective feelings acceptable/unacceptable
H-1	Male	38	174	72	0.5	20	Acceptable
H-2	Male	42	172	78	0.5	20	Acceptable
H-3	Male	30	176	70	0.5	20	Acceptable
H-4	Male	46	160	65	0.5	20	Acceptable
H-5	Female	28	160	57	0.5	20	Acceptable
H-6	Female	40	162	55	0.5	20	Acceptable
P-1	Male	20	175	62	0.2	20	Acceptable
P-2	Male	32	168	65	0.2	20	Acceptable

Figure 9 Example of healthy individuals and patients

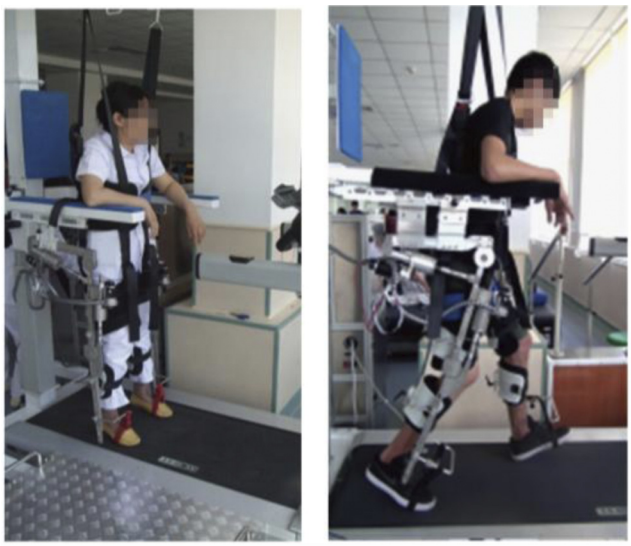

(a) **(b)**

Notes: (a) Healthy doctor; (b) one patient.

3.2 Results of patients

After 10 days of training, patients feel acceptable and the feasibility of LLERRS is confirmed. The robot provides assisted force to stand and walk, and normalization of gait planning is very useful to reconstruct a patient's gait.

As Figure 11(a) shows, position and velocity of hip and knee changed disorderly before 6 s. We find that response time exceeds 1.5 s. Moreover, movements of left and right legs are not consistent so that we could not find one gait cycle in the first 6 s. The time of one gait cycle in Figure 11(a) is about 3 s. As Figure 11(b) shows, most of the torque of right hip varies periodically, but with some abnormal points on the left side. As Figure 11(c) shows, torques of right knee and left knee have a time delay of 1.5 s, but left side shows good periodicity and one abnormal point is noted on the right side.

3.3 Results analysis

It is well known that thigh and crus in humans comprise an open-chain structure in terms of mechanics (Jin *et al.*, 2011), and the movement of hip is before the knee during walking. If one side of lower limb loses its ability to walk, the hip joint of this side will have no sense of autonomy, so the leg and exoskeleton will demonstrate good consistency. This study confirmed these, and the results of an healthy individual show 0.8 s response time, 1.8 s gait cycle time and 0.9 s time delay, which are all in the normal range. Also, cyclical movement of left leg and right leg confirms that the man's lower limbs have no direct problem. Although some deviation points appeared on the right and left sides (especially on the right side) in Figure 10(c), considering that the deviations are not large and the tester may not be familiar with the equipment, this situation is considered normal. Moreover, this study may indicate that both the left and right legs have independent consciousness, thereby proving that the two legs are healthy. Meanwhile, the results of patients show 1.5 s response time, 3 s gait cycle time and 1.5 s time delay, which are also reasonable. As Figure 11(b) shows, abnormal points on the left side imply that the left side was healthy, and torque of right side has good reproducibility and similar curves, so it may be accompanied with certain problems. As Figure 11(c) shows, one abnormal point was noted on the right side. Because movement of knee joint often happens after the hip joint for single leg when human walks from standing posture. If knee joint has problems, it is prone to have abnormal points. Combining Figure 11(b) with Figure 11(c), we suspected that the patient may have hemiplegia or the right lower limb may be the side with problem. To confirm this guess, the patient's pathology was reviewed. Finally, the study confirmed that the inference was correct, and the data are from the patient with encephalitis.

In addition, the study found that the peak velocity of the hip and knee for patient was lower than that under no load when comparing patient's data with no load (Figure 12). The reason is that patients can add additional motor load. Specific performances are described in Figure 12(a) and (b). In Figure 12(a), the velocity data with no load and patient showed some time delays. Maximum lags for left and right knees were 1.2 and 0.8 s, respectively, and maximum lags for left and right hips were 1 and 0.8 s, respectively. Simultaneously, the position data with no load and patient also have some time delays, which is consistent with Yang' study (Yang *et al.*, 2014). The maximum lags for position correspond with the abovementioned speed. Meanwhile, the response time for patients is significantly

Figure 10 Training results of one healthy volunteer

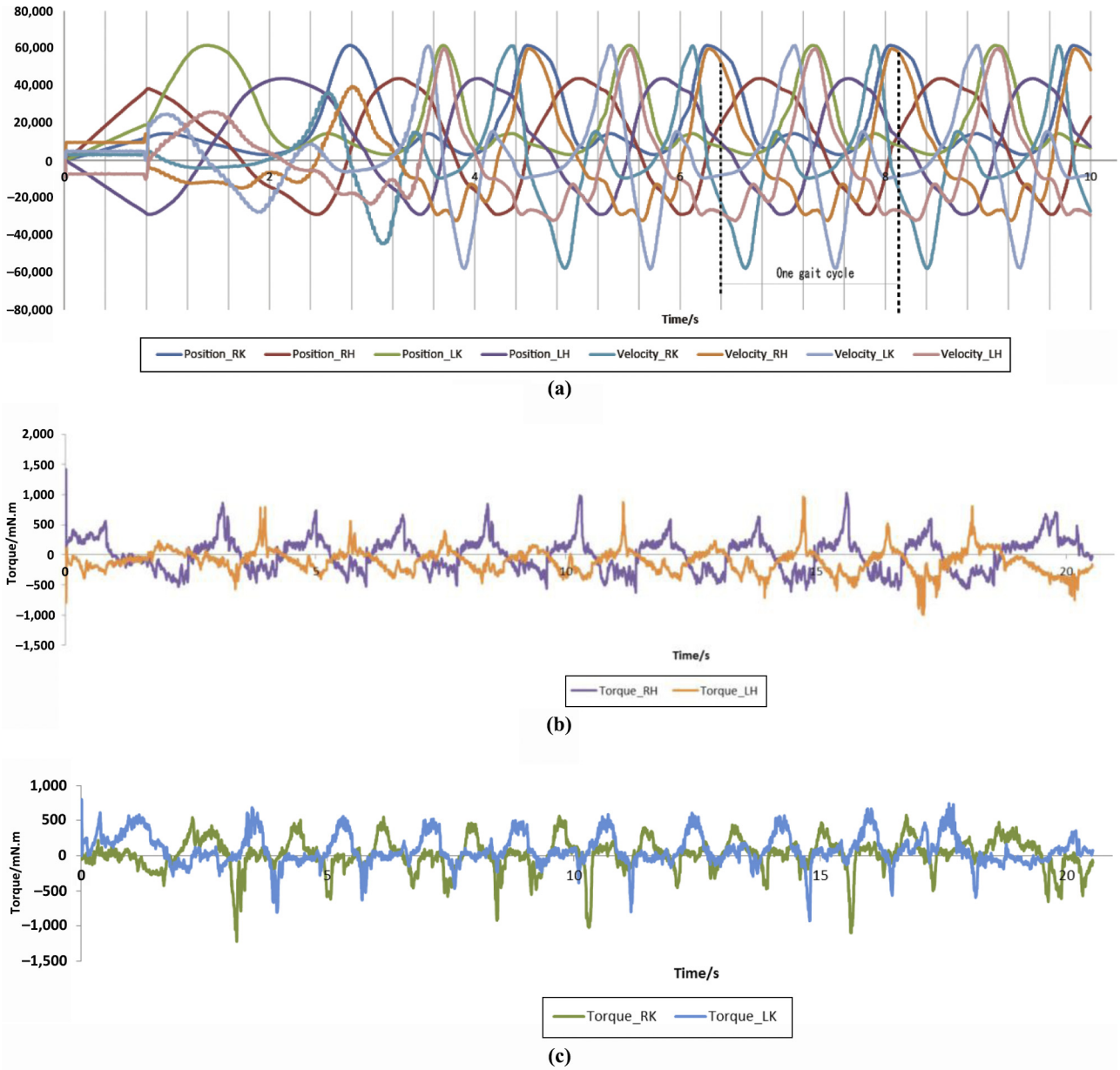

Notes: (a) Position and velocity data of hips and knees; (b) torque data of right and left hips; (c) torque data of data of right and left knees

greater than on load. All of these confirmed the feasibility and function of LLERRS.

Comparing patient's data [Figure 11(b)] with healthy individual's data [Figure 10(b)], we found that the biggest torque for the right hip of the healthy individual was about 1,490 mN·m, which was measured at the beginning of training. The biggest torque for the left hip was smaller than that for the right hip. Similarly, we found that the biggest torque for patient's right hip was about 1,000 mN·m, which was also determined at the beginning of training. The biggest torque for left hip was smaller than that of right hip. Theoretically, both right and left hips should have the same value when the robot is used by a healthy individual or patient. Thus, right joint of LLERRS may have friction, which should be improved. Through same comparison of knee data for normal individual [Figure 10(c)] and patient [Figure 11(c)], we found that left joint of LLERRS also exhibited friction. Because the maximum values for both normal individual and patient are in the range of 600-1100 mN·m when training lasted for a few seconds, the value of load on the exoskeletons was likely very similar. When we compared healthy individuals' weight (60.5 kg) with patient's weight (62 kg), we found that they were close. When the degree of weight loss was similar, above inference

Figure 11 Training results of one patient

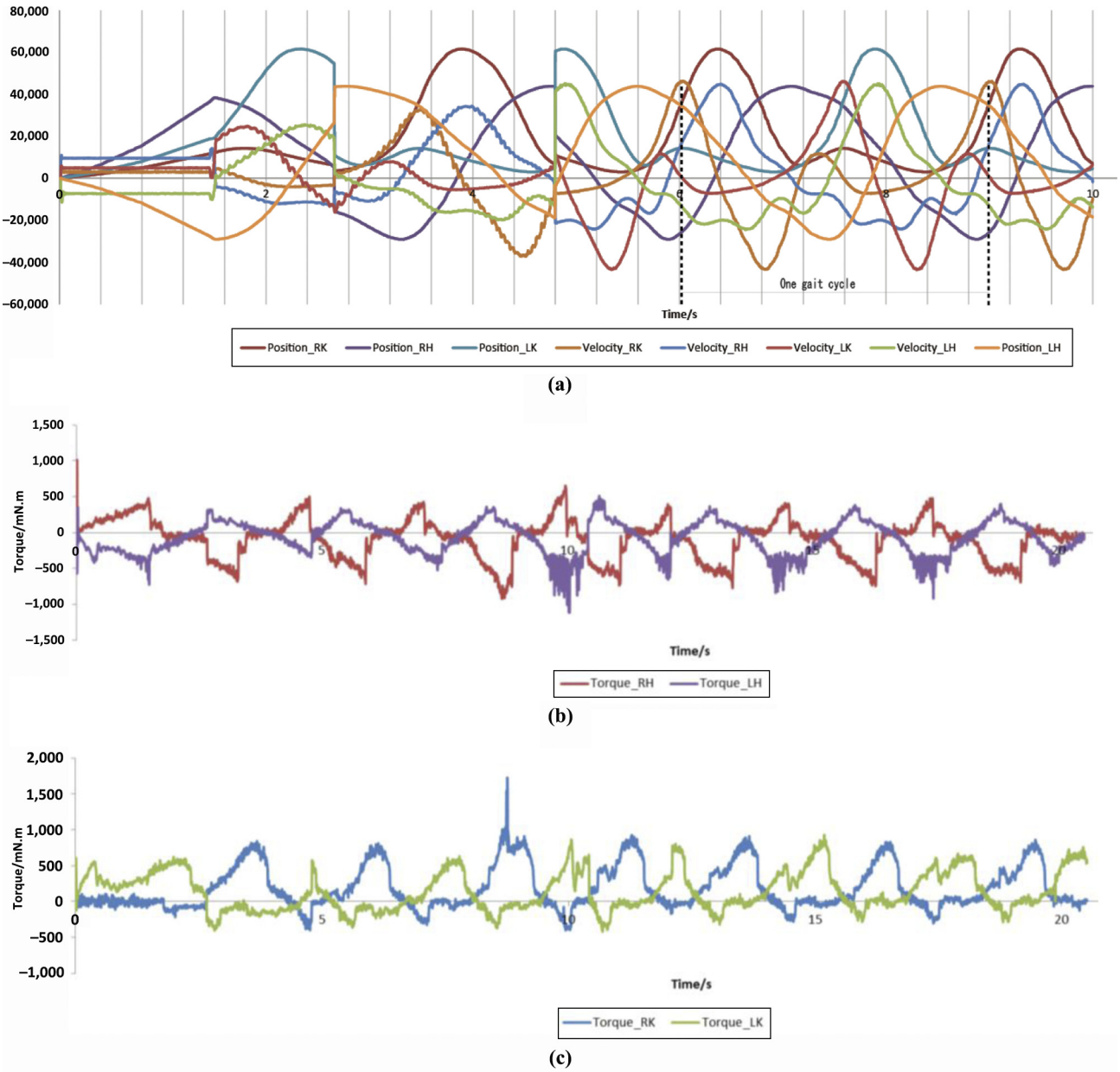

Notes: (a) Position and velocity data of hips and knees; (b) torque data of right and left hips; (c) torque data of right and left knees

was established. However, as shown in Figure 13(b), (c) and (d), most of data for healthy individual and patient have same trend. Although maximum, minimum and 75th are different, median and 25th have similar values. Figure 13(a) shows that right hip statistical data for healthy individual and patient have obvious difference. This phenomenon also describes that the right side may be the problem side indirectly, and it can be explained with open chain structure of lower limb. When one side of lower limb loses its function, respective side of the hip joint has a good consistency with exoskeleton, but knee will not show. These confirm sensitivity and reliability of the robot again.

4. Conclusion

In conclusion, a lower limb exoskeleton rehabilitation robot was developed to support standing/walking training. Details of structure and control system were described. Functional experiments were conducted on healthy individuals and patients. Experimental data were analyzed and discussed. Through prototype experiment, feasibility and function of the robot were confirmed, and performances on healthy individuals and patients are different and consistent with actual situation. LLERRS is simpler and more conducive to practical application. However, therapeutic effects need to be evaluated in the future, and more details should be improved continuously based on the actual demand.

Figure 12 Results of the patient and no load. The patient was the same as the one shown in Figure 11

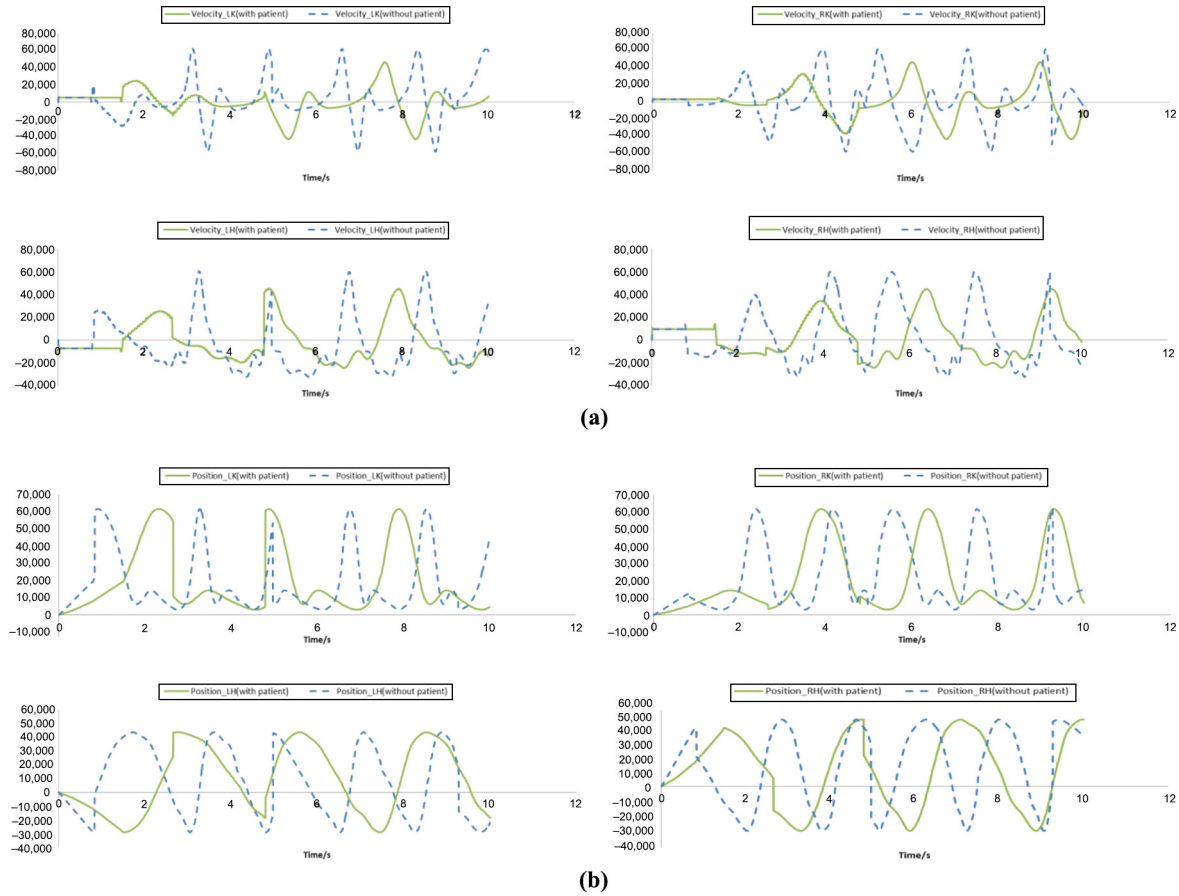

Notes: (a) Velocity trend of the joints for training and no load; (b) position trend of the joints for training and no load

Figure 13 Statistical analysis of torque for healthy individual and patient. It illustrates the maximum, minimum, median, 25th and 75th percentiles of the motor torque for hip joint and knee joint

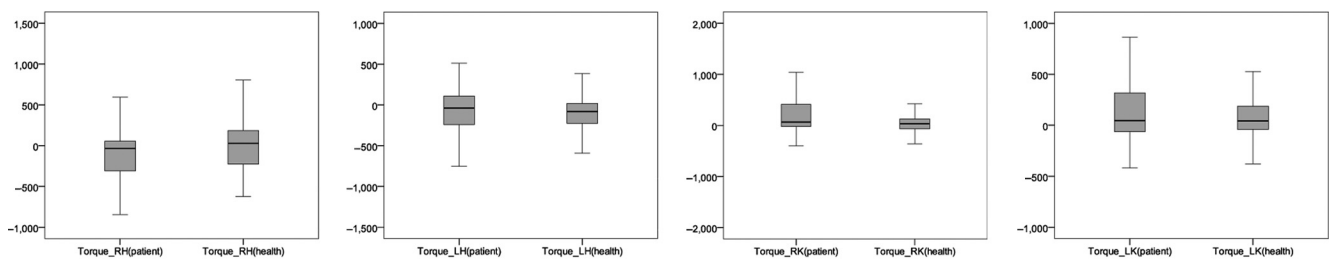

Notes: (a) Statistical analysis for right hip; (b) statistical analysis for left hip; (c) statistical analysis for right knee; (d) statistical analysis for left knee

References

Accoto, D., Carpino, G., Sergi, F., Tagliamonte, N.L., Zollo, L. and Guglielmelli, E. (2013), "Design and characterization of a novel high-power series elastic actuator for a lower limb robotic orthosis", *International Journal of Advanced Robotic Systems*, Vol. 10 No. 10359, pp. 1-12.

Banala, S.K., Kim, S.H., Agrawal, S.K. and Scholz, J.P. (2009), "Robot assisted gait training with Active Leg Exoskeleton (ALEX)", *IEEE Transactions on Neural Systems & Rehabilitation Engineering*, Vol. 17 No. 1, pp. 2-8.

Bonnyaud, C., Pradon, D., Boudarham, J., Robertson, J., Vuillerme, N. and Roche, N. (2014), "Effects of gait training using a robotic constraint (Lokomat®) on gait kinematics and kinetics IN chronic stroke patients", *Journal of Rehabilitation Medicine*, Vol. 46 No. 2, pp. 132-138.

Chen, D.S., Ning, M. and Zhang, B.G. (2015), "An improvement to the reciprocating gait orthosis for aiding

paraplegic patients in walking", *Science China-Technological Sciences*, Vol. 58 No. 4, pp. 727-737.

Chen, K., Liu, Q. and Wang, R. (2011), "Development of a body weight-support gait training robot", *Chinese Journal of Rehabilitation Medicine*, Vol. 26 No. 9, pp. 847-851.

Esquenazi, A., Talaty, M., Packel, A. and Saulino, M. (2012), "The rewalk powered exoskeleton to restore ambulatory function to individuals with thoracic-level motor-complete spinal cord injury", *American Journal of Physical Medicine & Rehabilitation*, Vol. 91 No. 11, pp. 911-921.

Geroin, C., Mazzoleni, S., Smania, N., Gandolfi, M., Bonaiuti, D., Gasperini, G., Sale, P., Munari, D., Waldner, A., Spidalieri, R., Bovolenta, F., Picelli, A., Posteraro, F., Molteni, F. and Franceschini, M. (2013) "Systematic review of outcome measures of walking training using electromechanical and robotic devices in patients with stroke", *Journal of Rehabilitation Medicine*, Vol. 45 No. 10, pp. 987-996.

Guo, Z., Yu, H.Y. and Yin, Y.H. (2014), "Developing a Mobile Lower Limb Robotic Exoskeleton for Gait Rehabilitation", *Journal of Medical Devices*, Vol. 8 No. 4, pp. 1-6.

Hussain, S., Xie, S.Q., Liu, G.Y. and Liu, G. (2011), "Robot assisted treadmill training: mechanisms and training strategies", *Medical Engineering & Physics*, Vol. 33 No. 5, pp. 527-533.

Hussain, S., Jamwal, P.K. and Ghayesh, M.H. (2016), "Single joint robotic orthoses for gait rehabilitation:an educational technical review", *Journal of Rehabilitation Medicine*, Vol. 48 No. 4, pp. 333-341.

Jezernik, S., Colombo, G., Keller, T., Frueh, H. and Morari, M. (2003), "Robotic Orthosis Lokomat: a rehabilitation and research tool", *Neuromodulation*, Vol. 6 No. 2, pp. 108-115.

Jin, D.W., Zhang, J.C., Wang, R.C., Wang, G.Z., Yang, J.K., Ji, L.H., Hao, Z.X., Gao, X.R. and Jia, X.H. (2011), *Bio-Mechanology in Rehabilitation Engineering*, Tsinghua University Press, Beijing.

Joanne, P. (2014), "The Pransky interview: Russ Angold, co-founder and president of Ekso™ Labs", *Industrial Robot: An International Journal*, Vol. 4 No. 4, pp. 329-334.

Kawamoto, H., Kamibayashi, K., Nakata, Y., Yamawaki, K., Ariyasu, R., Sankai, Y., Sakane, M., Eguchi, K. and Ochiai, N. (2013), "Pilot study of locomotion improvement using hybrid assistive limb in chronic stroke patients", *BMC Neurol*, Vol. 13 No. 1, pp. 93-98.

Krishnan, C., Ranganathan, R., Dhaher, Y.Y. and Rymer, W.Z. (2013), "A pilot study on the feasibility of robot-aided leg motor training to facilitate active participation", *Plos One*, Vol. 8 No. 10, pp. 1-8.

Li, W., Huang, Y., Xu, J. and He, J.P. (2011), "Brain activity during walking in patient with spinal cord injury", *International Symposium on Bioelectronics and Bioinformatics in Suzhou*, IEEE, New York, NY, pp. 96-99.

Lu, Q., Liang, J.X., Qiao, B. and Ma, O. (2013), "A New Active Body Weight Support System Capable of Virtually Offloading Partial Body Mass", *IEEE/ASME Transactions on Mechatronics*, Vol. 18 No. 1, pp. 11-20.

Onen, U., Botsali, F.M., Kalyoncu, M., Tinkir, M., Yilmaz, N. and Sahin, Y. (2014), "Design and actuator selection of a lower extremity exoskeleton", *IEEE/ASME Transactions on Mechatronics*, Vol. 19 No. 2, pp. 623-632.

Pan, D.L., Gao, F. and Miao, Y.J. (2014), "Dynamic research and analyses of a novel exoskeleton walking with humanoid gaits", *Proceedings of the Institution of Mechanical Engineers, Part C: Journal of Mechanical Engineering Science, Plos One*, Vol. 228 No. 9, pp. 1501-1511.

Sanz-Merodio, D., Cestari, M., Arevalo, J.C., Carrillo, X.A. and Garcia, E. (2014), "Generation and control of adaptive gaits in lower-limb exoskeletons for motion assistance", *Advanced Robotics*, Vol. 28 No. 5, pp. 329-338.

Stegal, P., Winfree, K., Zanotto, D. and Agrawal, S.K. (2013), "Rehabilitation Exoskeleton Design: Exploring the Effect of the Anterior Lunge Degree of Freedom", *IEEE Transactions on Robotics*, Vol. 29 No. 4, pp. 838-846.

Sui, J.F., Liu, Y.L., Yang, R.Z. and Ji, L.H. (2014), "A multiposture locomotor training device with force-field control", *Advances in Mechanical Engineering*, Vol. 6 No. 173518, pp. 1-10.

Wang, W.Q., Hou, Z.G., Tong, L.N., Zhang, F., Chen, Y.X. and Tan, M. (2014), "A novel leg orthosis for lower limb rehabilitation robots of the sitting/lying type", *Mechanism and Machine Theory*, Vol. 74, pp. 337-353.

Yan, H. and Yang, C.J. (2014), "Design and validation of a lower limb exoskeleton employing the recumbent cycling modality for post-stroke rehabilitations", *Proceedings of the Institution of Mechanical Engineers, Part C: Journal of Mechanical Engineering Science*, Vol. 228 No. 18, pp. 3517-3525.

Yang, W., Zhang, X.F., Yang, C.J. and WU H.J (2014), "Design of a lower extremity exoskeleton based on 5-bar human machine model", *Journal of Zhejiang University(Engineering Science)*, Vol. 48 No. 3, pp. 430-435.

Zhao, P. (2014), "Study on control strategy of lower limb rehabilitation robot based on EMG", Working paper, School of Electrical Engineering, Yanshan University, Qinghuangdao, May.

Further reading

Hussain, S. (2014), "State-of-the-art robotic gait rehabilitation orthoses: design and control aspects", *NeuroRehabilitation*, Vol. 35 No. 4, pp. 701-709.

Corresponding author

Diansheng Chen can be contacted at: chends@buaa.edu.cn